Copy No._____

Defence Research and Development Canada | Recherche et développement pour la défense Canada

DEFENCE R&D DÉFENSE

Capability of RADARSAT-1 for estimation of ocean surface current on the Scotian Shelf

D. Hutt
DRDC Atlantic

J. Stockhausen
Helical Systems, Dartmouth, NS

P. W. Vachon
DRDC Ottawa

D. Mosher
DRDC Atlantic

Defence R&D Canada – Atlantic

Technical Memorandum
DRDC Atlantic TM 2003-268
December 2003

Canada

Copy No:

Capability of RADARSAT-1 for estimation of ocean surface current on the Scotian Shelf

D. Hutt
DRDC Atlantic

J. Stockhausen
Helical Systems, Dartmouth, Nova Scotia

P. W. Vachon
DRDC Ottawa

D. Mosher
DRDC Atlantic

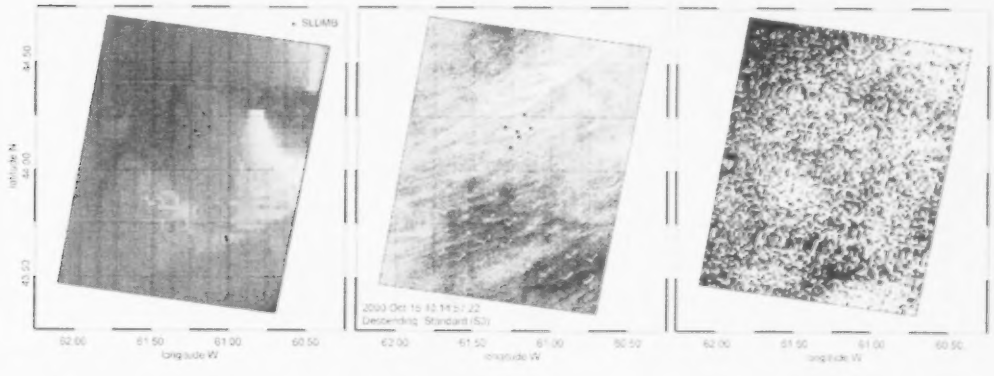

Defence R&D Canada – Atlantic

Technical Memorandum

DRDC Atlantic TM 2003-268

December 2003

Author

D. L. Hutt

Approved by

R. Kuwahara
Head, Signatures

Approved for release by

Kirk Foster
DRP Chair

© Her Majesty the Queen as represented by the Minister of National Defence, 2003
© Sa majesté la reine, représentée par le ministre de la Défense nationale, 2003

Abstract

Doppler shifts in space-based Synthetic Aperture Radar (SAR) data are due to movement of objects in the image area. These frequency shifts are most obvious in fast moving point targets such as ships. However, a distributed target such as the sea surface can also cause a measurable Doppler shift from which ocean surface currents can be estimated. We compare surface currents derived from three standard mode RADARSAT-1 scenes over the Scotian shelf to *in situ* currents measured with 21 Self-Locating Datum Marker Buoys (SLDMBs). The SLDMBs drift with the local surface current, and their locations, obtained every 30 minutes via Argos satellite, are used to calculate the current. Three RADARSAT-1 scenes were processed by Atlantis Scientific, of Ottawa, Canada to obtain the component of the surface current vector perpendicular to the path of the satellite. The results show that the noise in the derived Doppler shift was comparable to the Doppler shift expected from the relatively low surface currents prevalent on the Scotian Shelf. While it was concluded that present space-based SAR technology cannot provide accurate surface current data for Scotian Shelf conditions, the methodology and results provide a useful metric by which future SAR systems can be evaluated.

Résumé

Le décalage Doppler permet de mesurer le déplacement d'objets dans l'image captée par un radar à synthèse d'ouverture (RSO) satellisé. Ces décalages sont très évidents pour des cibles en déplacement rapide — les bateaux, par exemple. Toutefois, une zone-objectif étendue comme la surface de la mer produit également des décalages Doppler mesurables, à partir desquels on peut mesurer les courants océaniques de surface. Nous comparons les courants de surface au-dessus de la plate-forme Scotian, calculés à partir de trois scènes captées par RADARSAT-1, en mode normal, et ceux mesurés sur place, à l'aide de 21 bouées-repères électroniques autolocalisantes (BREAP). On a calculé le courant à partir des mesures de la position de bouées-repères dérivant dans le courant de surface par les satellites Argos, toutes les trente minutes. La société Atlantis Scientific d'Ottawa (Canada) a calculé la composante du vecteur vitesse du courant de surface perpendiculaire à la trajectoire du satellite, à partir des trois images scènes de RADARSAT-1. Les résultats montrent que le bruit dans le décalage Doppler calculé était comparable au décalage Doppler prévu pour les courants de surface relativement faibles au-dessus de la plate-forme Scotian. Bien que nous concluions que la technologie spatiale actuelle de RSO ne permet pas d'obtenir des données précises sur les courants de surface pour des conditions comme celles de la plate-forme Scotian, la méthodologie et les résultats nous donnent un critère utile à partir duquel on pourra évaluer les prochains systèmes RSO.

This page intentionally left blank.

Executive summary

Background

Numerical ocean models have the potential to forecast water current and density fields for operational use by the Canadian Forces. The models must be constrained by environmental inputs to ensure physically reasonable solutions. One environmental parameter that has a high information content for the purpose of ocean modelling is the surface current field. While land-based high-frequency radar has been used to measure surface currents in coastal areas over the past decade, there is no operational space-based method for measuring surface currents.

Experiment

Previous work has shown that surface currents can be estimated from space-based Synthetic Aperture Radar (SAR) data by measuring Doppler frequency shifts in different parts of the image scene. In this paper we compare surface currents derived from three standard mode RADARSAT-1 SAR scenes over the Scotian shelf to in situ currents measured with 21 Self-Locating Datum Marker Buoys (SLDMBs). The SLDMBs drift with the local surface current, and their locations, obtained every 30 minutes via Argos satellite, are used to calculate the current. Only the component of the surface current vector perpendicular to the path of the satellite can be resolved. The processing of the images for the surface current product was done by Atlantis Scientific, Ottawa, Canada.

Results

The results show that the noise in the derived Doppler shift was comparable to the Doppler shift expected from the relatively low surface currents prevalent on the Scotian Shelf. Therefore it was concluded that present space-based SAR technology cannot provide accurate surface current data for Scotian Shelf conditions. However, the methodology and results provide a useful metric by which future SAR systems can be evaluated.

The work was done in an effort to evaluate the potential for using space-based SAR data for remote sensing of surface currents. Future work will include a similar experiment to estimate surface currents in the Nova Scotia and Labrador currents using both RADARSAT-1 and the ENVISAT ASAR sensor.

Hutt, D., Stockhausen, J., Vachon, P. W., Mosher, D., 2003. Capability of RADARSAT-1 for estimation of ocean surface current on the Scotian Shelf. DRDC Atlantic TM 2003-268. Defence R&D Canada – Atlantic.

Sommaire

Context

Les modèles océaniques numériques ont le potentiel de prédire les champs de courant et de densité de l'eau en vue de l'utilisation opérationnelle par les Forces canadiennes. Ces modèles doivent être soumis à des contraintes environnementales pour donner lieu à des solutions physiquement faisables. Un des paramètres environnementaux qui apporte beaucoup d'information aux fins de la modélisation océanique est le champ de courant de surface. Bien que le radar haute fréquence terrestre ait été utilisé pour mesurer les courants de surface en zone littorale au cours de la dernière décennie, il n'existe pas de méthode opérationnelle pour mesurer les courants de surface à partir de l'espace.

Expérience

Il a été démontré que les courants de surface peuvent être estimés à partir de données d'un radar spatial à antenne synthétique (RAS) en mesurant les décalages Doppler à différentes parties de la scène image. Dans le présent rapport, nous comparons les courants de surface dérivés de trois scènes RAS de Radarsat-1 en mode standard au-dessus de la Plate-forme Scotian avec des courants sur place mesurés au moyen de 21 bouées-repères électroniques d'auto-positionnement (BREAP). Les BREAP dérivent selon le courant de surface local, et leurs emplacements, obtenus toutes les 30 minutes via un satellite Argos, sont utilisés pour calculer le courant. Seule la composante du vecteur de courant de surface perpendiculaire à la trajectoire du satellite peut être résolue. Le traitement des images en vue du produit de courants de surface a été effectué par Atlantis Scientific d'Ottawa, Canada.

Résultats

Les résultats montrent que le bruit dans le décalage Doppler dérivé était comparable au décalage Doppler attendu des courants de surface relativement faibles propres à la Plate-forme Scotian. Par conséquent, on a conclu que la technologie actuelle à RAS spatial ne peut pas fournir de données de courant de surface précises pour les conditions de la Plate-forme Scotian. Toutefois, la méthodologie et les résultats constituent des paramètres utiles pour évaluer les systèmes RAS futurs.

Le travail a été effectué dans le but d'évaluer le potentiel des données de RAS spatial utilisées pour la télédétection de courants de surface. Le travail futur comprendra une expérience semblable pour estimer les courants de surface au large de la Nouvelle-Écosse et du Labrador au moyen de Radarsat-1 et du capteur ASAR d'Envisat.

Hutt, D., Stockhausen, J., Vachon, P. W., Mosher, D., 2003. Capability of RADARSAT-1 for estimation of ocean surface current on the Scotian Shelf (Capacité de RADARSAT-1 pour l'estimation du courant de surface à la Plate-forme Scotian). RDDC Atlantique TM 2003-268. R et D pour la défense Canada – Atlantique.

Table of contents

Abstract i

Résumé i

Executive summary iii

Sommaire iv

Table of contents v

List of figures vi

List of tables vi

Acknowledgements vii

Introduction 1

2. Experimental data 3

2.1 RADARSAT-1 data 3

2.2 SLDMB data 4

3. Methodology 9

4. Results 16

5. Summary 20

References 21

Distribution list 22

105-04559/

List of figures

Figure 1.1 RADARSAT-1 SAR image of a ship and its wake 1
Figure 2.1 A SLDMB being deployed from research vessel Quest, Oct. 14, 2000 5
Figure 2.2 Deployment pattern used for SLDMBs during trial Q255. 5
Figure 2.3 Example of drift speed and direction data from SLDMB 17973 7
Figure 2.4 Drift patterns for SLDMBs deployed on Oct. 14 and Oct. 21, 2000. 8
Figure 3.1a RADARSAT image area for the 15 Oct. 2000 overpass 10
Figure 3.1b SLDMBs on SAR backscatter image, 15 Oct. 2000 11
Figure 3.2a RADARSAT image area for the 21 Oct. 2000 overpass 12
Figure 3.2b SLDMBs on SAR backscatter image, 21 Oct. 2000 13
Figure 3.3a RADARSAT image area for the 22 Oct. 2000 overpass 14
Figure 3.3b SLDMBs on SAR backscatter image, 22 Oct. 2000 15
Figure 4.1 Scatter plots of remotely sensed and *in situ* currents 19

List of tables

Table 2-1 RADARSAT-1 overpass times and modes during Q255 3
Table 2-2 Summary of SLDMB deployment information for Oct. 14 6
Table 2-3 Summary of SLDMB deployment information for Oct. 21 6
Table 3-1 SLDMB positions for RADARSAT overpass 15 October 2000 10
Table 3-2 SLDMB positions for RADARSAT overpass 15 October 2000 12
Table 3-3 SLDMB positions for RADARSAT overpass 15 October 2000 14
Table 4-1 *in situ* and remotely sensed surface currents, October 15, 2000 17
Table 4-2 *in situ* and remotely sensed surface currents, October 21, 2000 18
Table 4-3 *in situ* and remotely sensed surface currents, October 22, 2000 18

Acknowledgements

The authors would like to thank the following people for their contribution to this study:

- Commanders and crew of MPA Squadrons 415 and 405 of 14 Wing Greenwood, Nova Scotia for successful deployment of the SLDMBs.
- Master and crew of research vessel CFAV Quest for their excellent technical support during trial Q255.
- Dr. Marco Van der Kooij, Atlantis Scientific, Ottawa, Canada for helpful discussion and assistance with interpretation of the results of the SAR surface current extraction.
- Mr. John Wolfe, Canada Centre for Remote Sensing for processing of RADARSAT-1 raw data to image, ship and wind products.

1. Introduction

Motion of objects in the image area of a Synthetic Aperture Radar (SAR) scene result in Doppler shift of the SAR data. Such shifts are manifest in the image as a displacement of the moving object. This effect is well known in SAR images of relatively fast moving point targets, such as ships, where the SAR image of the ship can be seen to be displaced from its wake. An example of such an image is shown in Fig. 1.1. The speed of the moving target can be determined from the combination of a measurement of the offset and a number of orbital parameters. The mathematics were first fully described by Raney in 1971 [Ref. 1].

A distributed target can also cause Doppler shift in a SAR image if it is moving during the acquisition time of the image. Thus, in principle, ocean surface currents should be measurable if their Doppler shift can be detected and measured in the SAR data.

Efforts to extract ocean surface currents from space-based SAR data began with Shuchman [Ref. 2] who used data from SEASAT obtained in 1978. Unfortunately, the L-band SEASAT satellite was short lived, surviving for only 101 days. Shuchman attempted to extract ocean current information from SEASAT images of the ocean surface, but the Doppler shifts were too small in L-band to be measured using the Doppler Centroid estimation techniques of the day [Ref. 3].

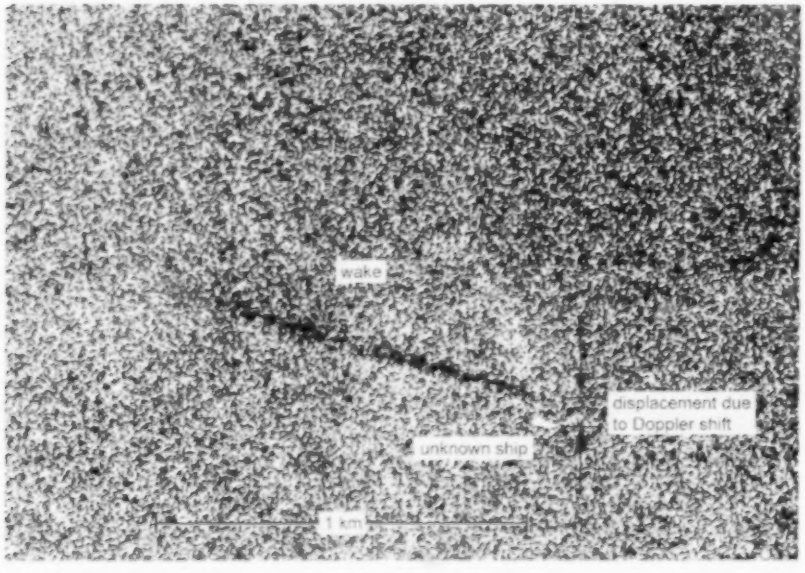

Figure 1.1 RADARSAT-1 SAR image of a ship and its wake. The image of the ship is displaced from the vertex of its wake as a result of its velocity relative to the background of the scene. The image is from a Standard mode 2 beam acquired May 3, 2001 near 39.3 deg N, 72.5 deg W off the coast of New Jersey.

Recently, Van der Kooij et al. [Ref. 3] demonstrated successful surface current extraction from C-band RADARSAT-1 and ERS-1 data over the Gulf Stream. A spatial resolution of 1-2 km with a precision of 0.2-0.3 m/s was achieved. Validation of the results was accomplished by comparing the remotely sensed currents to those obtained from a ship-mounted Acoustic Doppler Current Profiler (ADCP).

In the present study the methodology of Van der Kooij et al. is applied to a set of RADARSAT-1 scenes of the Scotian Shelf. The processing for surface current product was done by Atlantis Scientific, Ottawa, Canada. The remotely sensed currents are compared to *in situ* measurements obtained from a set of drifting Self Locating Datum Marker Buoys (SLDMBs). The work was done in an effort to evaluate the potential for using remotely sensed surface currents as input data for an oceanographic model of the Scotian Shelf.

High quality remotely sensed measurements of sea surface temperature and winds are standard oceanographic data products that are widely available for assimilation into numerical ocean models. However, ocean currents provide better information content for models than temperature or winds. Therefore, a means to remotely sense ocean currents from space would be an extremely valuable resource for the ocean modelling community.

2. Experimental data

RADARSAT-1 images, and SLDMB surface current measurements were obtained during scientific cruise Q255 of DRDC Atlantic's research vessel *Quest* in October, 2000. A variety of experiments to characterize the physical and acoustic properties of the sea surface, water column and seabed were performed in the vicinity of 44 deg. N, 061 deg. W, approximately 100 km west of Sable Island on the Scotian Shelf.

2.1 RADARSAT-1 data

RADARSAT-1 data was ordered through the RADARSAT Order Desk at the Canada Centre for Remote Sensing. The available beams for a given time and geographical area were predicted using the Swath Planning Application (SPA) distributed by RADARSAT International (RSI), which is a Windows application that models the satellite's orbital dynamics. Once a scene is selected by the user, the SPA saves a description of the scene to a file which is forwarded to the order desk via e-mail.

RADARSAT-1 images that are requested are not always available for a variety of reasons. Scenes ordered by Canadian federal government agencies (such as DRDC Atlantic) for routine purposes have a lower priority than scenes ordered by corporate clients or scenes required for operational or emergency applications such as ice or flood monitoring. It takes a few seconds for the satellite's radar to change mode between acquisitions, so scenes ordered by one client can preclude acquisition of a scene by another. For Q255, seven scenes were ordered and all were obtained. The times and beam modes for each RADARSAT-1 scene are summarized in Table 2-1

The SAR data was received and processed to RAW format by the Canadian Data Processing Facility (CDPF) in Gatineau, PQ and sent to DRDC Atlantic on compact disc media. The files were processed to SGF image products in CEOS format using the Advanced Precision Processor (APP), a workstation-based SAR processor. An ADC saturation power loss correction algorithm was used during processing. The CEOS data products were subsequently processed through the Ocean Monitoring Workstation (OMW) wind and ship detection modules. Wind and ship results are reported in Ref. 4.

Table 2-1 RADARSAT-1 overpass times and modes during Q255

Date	Time (UTC)	Mode
October 11, 2000	21:51:14	S2/Ascending
October 12, 2000	10:02:19	S7/Descending
October 14, 2000	22:03:42	S6/Ascending
October 15, 2000	10:14:53	S3/Descending
October 18, 2000	21:47:02	S1/Ascending
October 21, 2000	21:59:34	S5/Ascending
October 22, 2000	10:10:39	S5/Descending

The best results for Doppler shift detection in SAR imagery are obtained for images with moderate incidence angles. Therefore, of the seven images collected during the trial, the three with incidence angles between 30° and 42° were selected for processing for surface current. These images were the ones acquired on October 15, 21 and 22 with beam modes S3, S5 and S5, respectively. These standard modes have incidence angle ranges of 30°-37° (S3) and 36°-42° (S5).

2.2 SLDMB data

One of the greatest difficulties with search and rescue operations at sea is the rapid growth of the search area, due to the uncertainty of how life rafts or persons in the water drift in response to the prevailing winds and currents. Within a few hours the search area can become so large that an effective search is much more difficult.

The Self Locating Datum Marker Buoy (SLDMB) was developed by Seimac Ltd., Dartmouth Nova Scotia and DRDC Atlantic as a solution to this problem. During a Search and Rescue operation, SLDMBs are deployed from an Aurora or Hercules aircraft near a ship in distress. Upon entering the water, the buoys deploy in one of two selectable configurations which simulate the drift of a person in the water (PIW mode) or the drift of a life raft (LR mode). The drift pattern of a SLDMB in PIW mode is primarily influenced by ocean currents in the top 1 m of water. Therefore, for the purposes of this report, the drift speed and direction of a SLDMB in PIW mode is taken to be equivalent to that of the surface current.

The SLDMB contains a Global Positioning System (GPS) receiver which determines the buoy's geographical position, and an ARGOS transmitter, which relays the buoy position to a land station over the ARGOS satellite network. The information is then sent to the Rescue Coordination Center (RCC) in Halifax, Nova Scotia, which is in charge of Search and Rescue operations. By plotting the trajectory of the SLDMB over time, the RCC can estimate the probable location of survivors, and focus the search in that area.

The SLDMBs used for the Q255 experiment were provided by DRDC Atlantic and the Canadian Coast Guard (CCG). Twenty SLDMBs were deployed from Marine Patrol Aircraft (MPA) during flights on October 14 and 21, 2000. Five SLDMBs were deployed from *Quest*. All of the aircraft-deployed SLDMBs were in PIW mode. Of the five deployed from *Quest*, three were in PIW mode and two were in LR mode. SLDMBs from manufacture lots 002 and 007 were used for the October 14 and 21deployments, respectively. Figure 2.1 shows one of the authors (Mosher) deploying a SLDMB from Quest during the trial.

The aircraft deployed SLDMBs in groups of five in the cross pattern shown in Fig. 2.2. The cross pattern allows overall currents to be measured as well as dispersion from the initial deployment site. On Oct.14, 2000 a MPA from 415 Squadron deployed five SLDMBs at site 2 and at site 4. A MPA from 405 Squadron deployed five SLDMBs each at sites 3 and 4 on Oct. 21, 2000. It was requested that the MPA crew note the Global Positioning System (GPS) drop time and locations for each SLDMB. Information on the deployment of all SLDMBs is summarized in Tables 2-2 and 2-3.

In addition to providing surface current measurements, the large number of SLDMBs deployed during Q255 provided an opportunity to evaluate their reliability and for MPA air crew to practice the air deployment procedure.

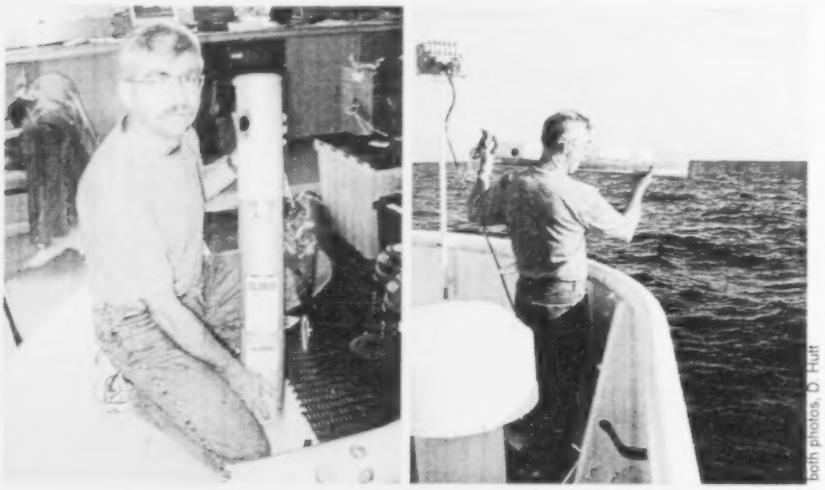

Figure 2.1 Author Don Mosher prepares a SLDMB for deployment (left) and deploys it from the quarterdeck of research vessel Quest, Oct. 14, 2000.

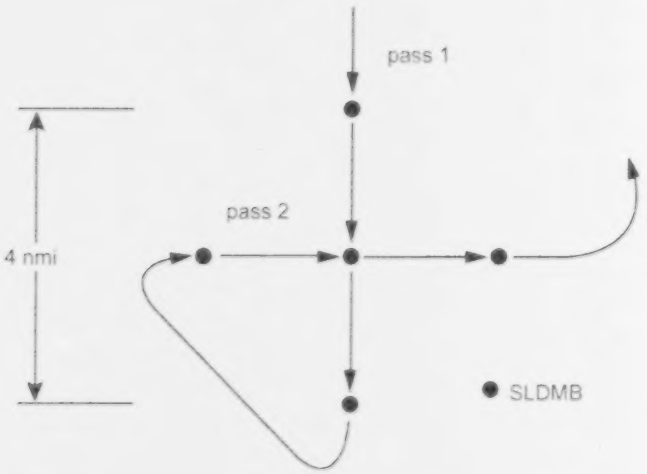

Figure 2.2 Deployment pattern used for SLDMBs during Q255.

Table 2-2 Summary of SLDMB deployment information for Oct. 14, 2000

ARGOS ID	Q255 site	deployed from	time (utc)	lat N	lon W	mode	comments
17302	2	MPA	16:55	43 39.47	60 58.30	PIW	U/S
2332	4	QUEST	13:03	44 05.25	61 17.04	LR	terminates Oct.19
2333	4	QUEST	13:06	44 05.31	61 17.04	PIW	terminates Oct.19
17751	2	MPA	16:56	43 37.60	60 59.37	PIW	terminates Oct.18
17752	2	MPA	16:57	43 35.71	61 00.50	PIW	U/S
17846	2	MPA	16:59	43 36.42	60 57.27	PIW	terminates Oct.19
17847	2	MPA	17:01	43 38.53	61 01.83	PIW	U/S
17969	4	MPA	17:57	44 02.50	61 10.40	PIW	U/S
17970	4	MPA	19:04	44 04.80	61 16.30	PIW	terminates Oct.19
17971	4	MPA	18:00	44 07.30	61 22.40	PIW	terminates Oct.19
17972	4	MPA	18:04	44 00.20	61 19.32	PIW	terminates Oct.19
17973	4	MPA	18:06	44 08.90	61 12.90	PIW	terminates Oct.19

Table 2-3 Summary of SLDMB deployment information for Oct. 21, 2000

ARGOS ID	Q255 site	deployed from	time (utc)	lat N	lon W	mode	comments
02391	1	QUEST	13:23	44 09.34	61 10.57	LR	terminates Oct. 26
17309	1	QUEST	13:25	44 09.35	61 10.55	PIW	terminates Oct. 26
17311	1	QUEST	14:08	44 09.89	61 10.10	PIW	terminates Oct. 26
19268	3	MPA	17:41	44 26.94	61 34.68	PIW	terminates Nov. 30
19276	3	MPA	17:46	44 25.50	61 33.66	PIW	terminates Nov. 22
19281	3	MPA	17:44	44 23.58	61 33.60	PIW	terminates Nov. 25
19290	3	MPA	17:45	44 25.98	61 29.22	PIW	terminates Nov. 13
19291	3	MPA	17:49	44 25.38	61 37.80	PIW	terminates Nov. 30
19292	4	MPA	19:07	44.19.02	61 13.86	PIW	terminates Dec. 5
19311	4	MPA	19:10	44 11.22	61 03.84	PIW	terminates Nov. 24
19312	4	MPA	19:21	44 02.88	60 55.14	PIW	terminates Dec. 2
19314	4	MPA	19:20	44 15.30	60 54.54	PIW	terminates Nov. 21
19487	4	MPA	19:25	44 05.10	61 18.54	PIW	terminates Oct. 30

Of the 25 SLDMBs deployed during the trial, 21 were serviceable and provided valid data. On Oct. 14, four of the twelve SLDMBs deployed failed to operate. All of the 13 SLDMBs deployed on Oct. 21 were serviceable.

The SLDMBs deployed on Oct.14 were all from manufacture lot 002. The remaining inventory of lot 002 SLDMBs were quarantined as a result of the unacceptably high failure rate. All the SLDMBs deployed from the MPA on Oct.21 were from lot 007 and had been modified to increase the location logging rate from once per hour to once every 20 minutes. The self-scuttle feature was also disabled so that the buoys continued to function until their batteries ran out rather than scuttle after the usual five days. Most of the lot 007 SLDMBs lasted more than a month and one failed on Dec. 5, 2000 after 45 days of service.

There were minor gaps in some of the SLDMB data sets of the lot 007 buoys deployed on Oct. 21. The gaps are believed to be due to overflow of the SLDMBs memories during periods when there was an unusually long time between overpasses of NOAA satellites with the ARGOS receivers.

Of the SLDMBs deployed, eight were within the imaging area of the Oct. 15 RADARSAT-1 pass, while thirteen were within the Oct. 21 and 22 SAR scenes. *In situ* surface current data was extracted from the time-series of recorded positions for each SLDMB. A plot of drift speed and direction for one of the SLDMBs is shown in Fig. 2-3. It can be seen that the drift pattern is dominated by the circular tidal flow characteristic of shallow areas of the Scotian Shelf.

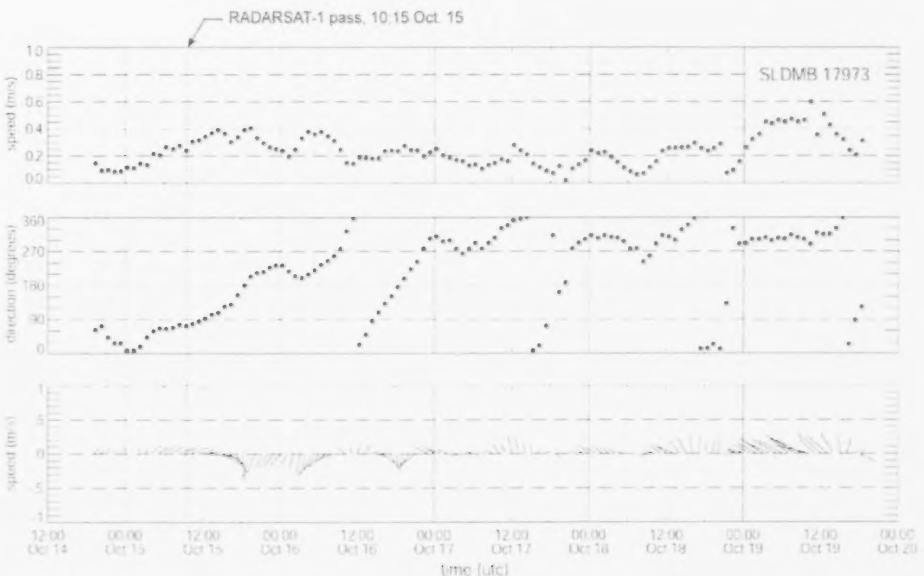

Figure 2.3 Example of drift speed and direction data from SLDMB 17973.

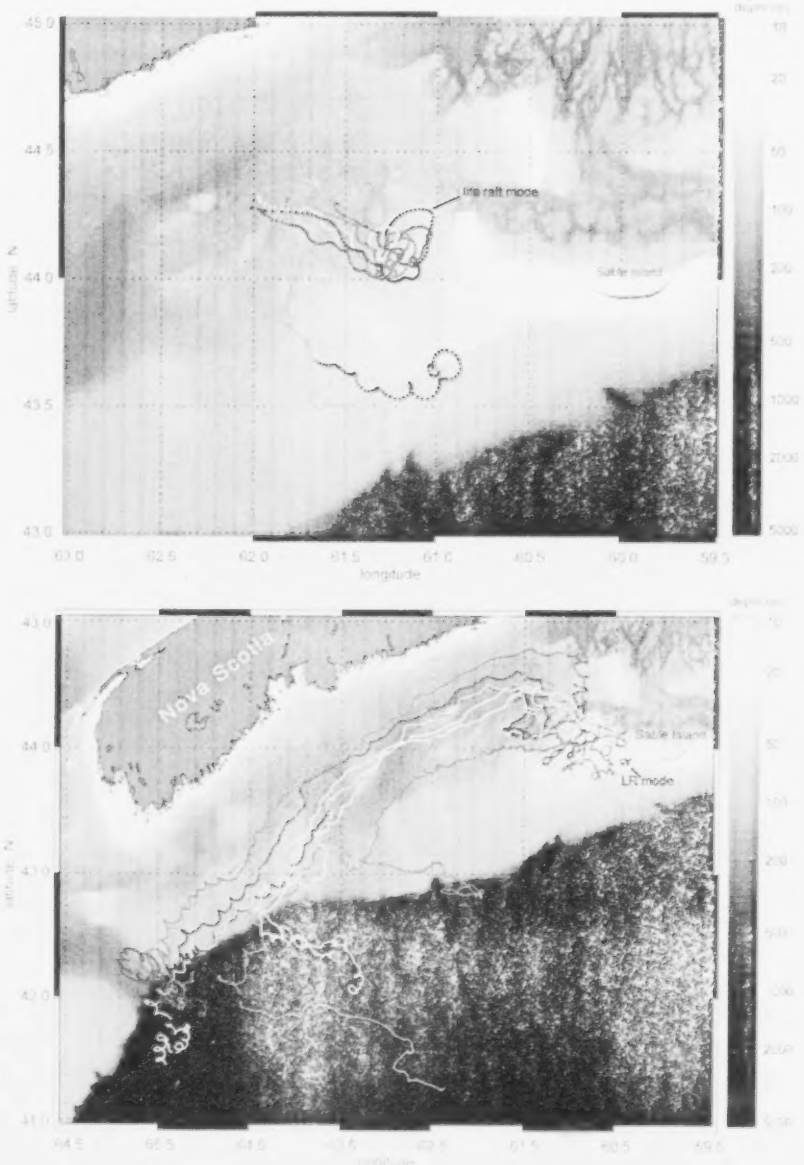

Figure 2.4 Drift patterns for SLDMBs deployed on Oct. 14, 2000 (top) and Oct. 21, 2000 (bottom). The Oct. 14 SLDMBs scuttled automatically after five days. The Oct. 21 SLDMBs were allowed to function until their batteries ran down. One lasted 45 days, hence the much longer trajectories evident in the bottom figure.

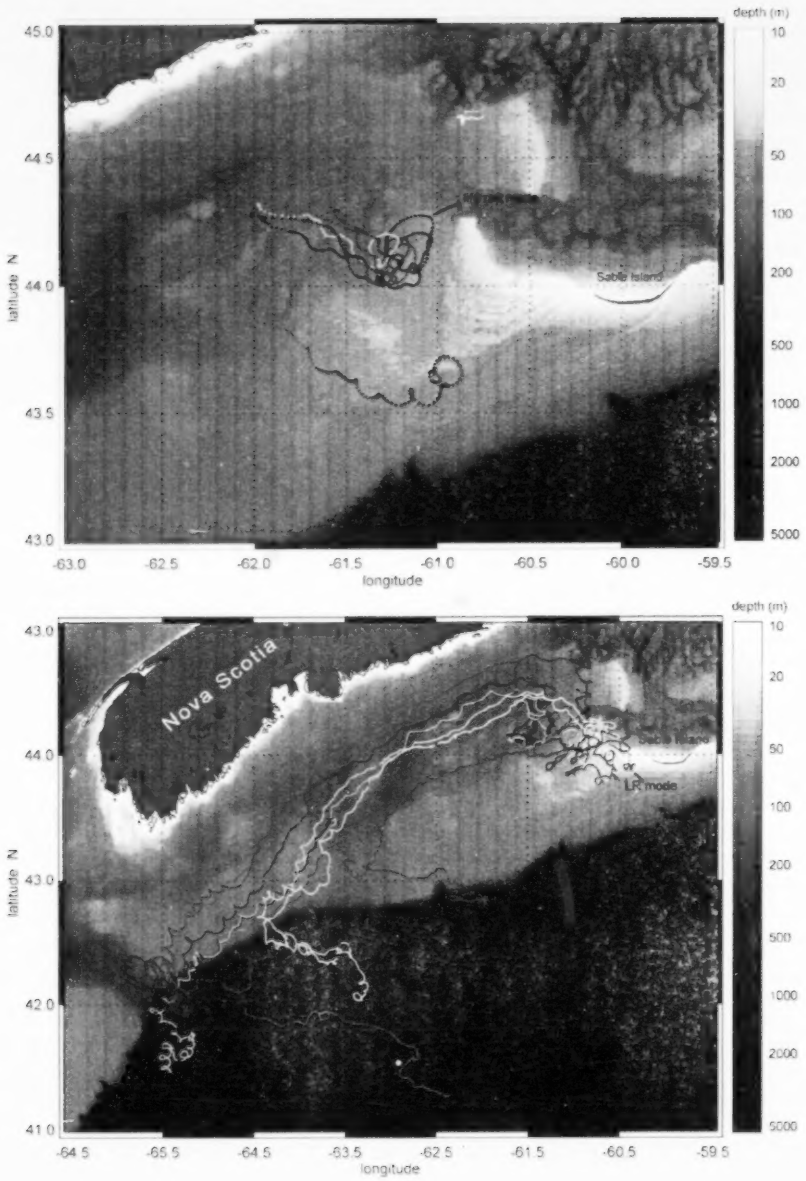

Figure 2.4 Drift patterns for SLDMBs deployed on Oct. 14, 2000 (top) and Oct. 21, 2000 (bottom). The Oct. 14 SLDMBs scuttled automatically after five days. The Oct. 21 SLDMBs were allowed to function until their batteries ran down. One lasted 45 days, hence the much longer trajectories evident in the bottom figure.

3. Methodology

The raw RADARSAT-1 data was processed by Atlantis Scientific, of Ottawa, Ontario to produce surface current values using the frequency shift technique described in Ref. 3. The process divides the image area into "patches" of data with areas approximately 1 x 1 km. The resultant velocities for each patch are the component of the true surface current that is perpendicular to the path of the satellite, as this is the only direction in which the Doppler shift can be measured. The resultant data product is a two dimensional array of Doppler centroid estimates for the three sets of SAR data provided to Atlantis.The processing steps described in Ref. 3 are as follows:

1. Generation of a Single Look Complex (SLC) image.
2. Calculation of a grid of Doppler Centroid estimates for overlapping patches of typically 64 (range) by 512 (azimuth) samples.
3. Removal of the Doppler Centroid component corresponding to non-moving terrain (if any).
4. Conversion of residual Doppler Centroid estimates to current velocity values using scene geometry.

Further processing of the remotely sensed current data was then carried out by author Stockhausen using the PCI suite of image analysis tools. Details of this analysis may be found in Ref. 5. First, the current data image was georeferenced using the four corner latitude and longitude coordinates provided by Atlantis Scientific. Then the current image was resampled at a higher spatial resolution using nearest neighbor interpolation in order to compensate for translational errors of up to 1/2 pixel caused by the georeferencing process. Finally, the remotely sensed current values were extracted from the image at the positions corresponding to SLDMB locations.

Figures 3.1a to 3.3a show the outlines of the acquired RADARSAT-1 scenes and the locations of the SLDMBs at the time of the satellite overpasses. Figures 3.1b to 3.3b show the corresponding georeferenced remotely sensed surface current components derived from the SAR image.The current values are displayed as a grey scale where black indicates westward flow and white indicates eastward flow.

Figures 3.1b to 3.3b also show the sea surface wind fields derived from the SAR data. The wind retrieval was based on the approach of Vachon and Dobson (Ref. 6), but using low (25 km) resolution wind directions measured by QuickScat. The QuickScat overpasses occurred within one hour of the RADARSAT-1 overpasses.

To compare the remotely sensed and *in situ* surface currents, the components of measured currents perpendicular to the satellite headings was determined. This required the satellite headings which were calculated from the corner coordinates of the current images. The resultant satellite paths for the overpasses of Oct. 15, 21 and 22 were 190.97°, 169.82° and 190.17°, respectively. These values were used to determine the perpendicular components of the *in situ* current values.

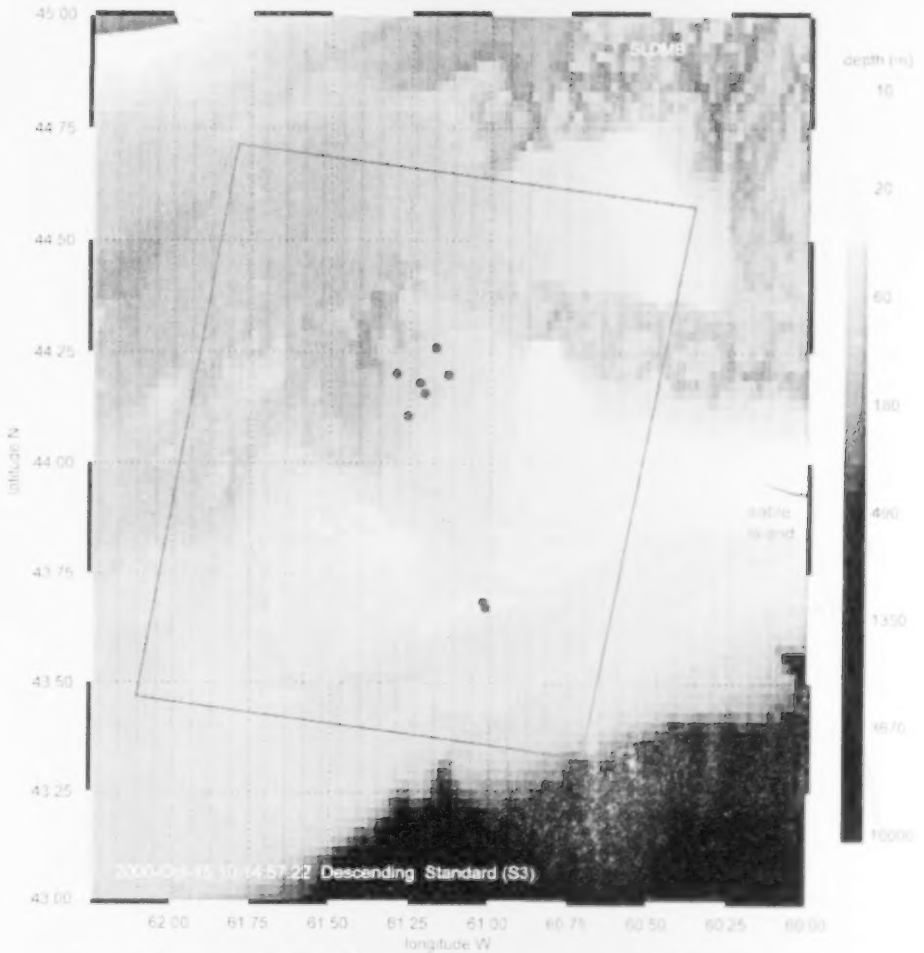

Figure 3.1a Outline of RADARSAT image area and positions of SLDMBs overlaid on bathymetry for the 15 Oct 2000 overpass

Table 3-1 SLDMB positions for RADARSAT overpass 15 October 2000

SLDMB (ID)	time (utc) hh:mm:ss	lat N	lon W
17751	10 03 00	43.684	-61.020
17846	10 01 00	43.671	-61.012
17970	10 06 00	44.156	-61.204
17971	10 05 00	44.201	-61.292
17972	10 06 00	44.106	-61.257
17973	10 06 00	44.198	-61.131
2332	10 01 00	44.259	-61.169
2333	10 02 00	44.180	-61.218

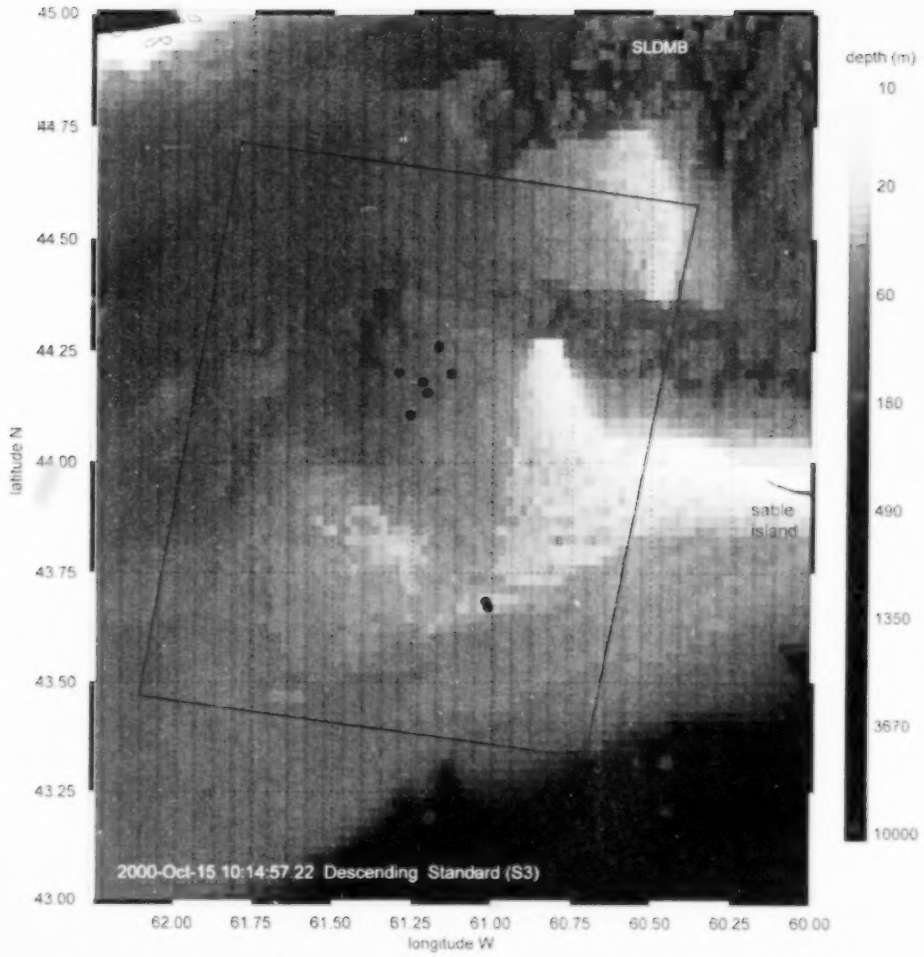

Figure 3.1a Outline of RADARSAT image area and positions of SLDMBs overlaid on bathymetry for the 15 Oct. 2000 overpass.

Table 3-1 SLDMB positions for RADARSAT overpass 15 October 2000

SLDMB (ID)	time (utc) hh:mm:ss	lat N	lon W
17751	10:03:00	43.684	-61.020
17846	10:01:00	43.671	-61.012
17970	10:06:00	44.156	-61.204
17971	10:05:00	44.201	-61.292
17972	10:06:00	44.106	-61.257
17973	10:06:00	44.198	-61.131
2332	10:01:00	44.259	-61.169
2333	10:02:00	44.180	-61.218

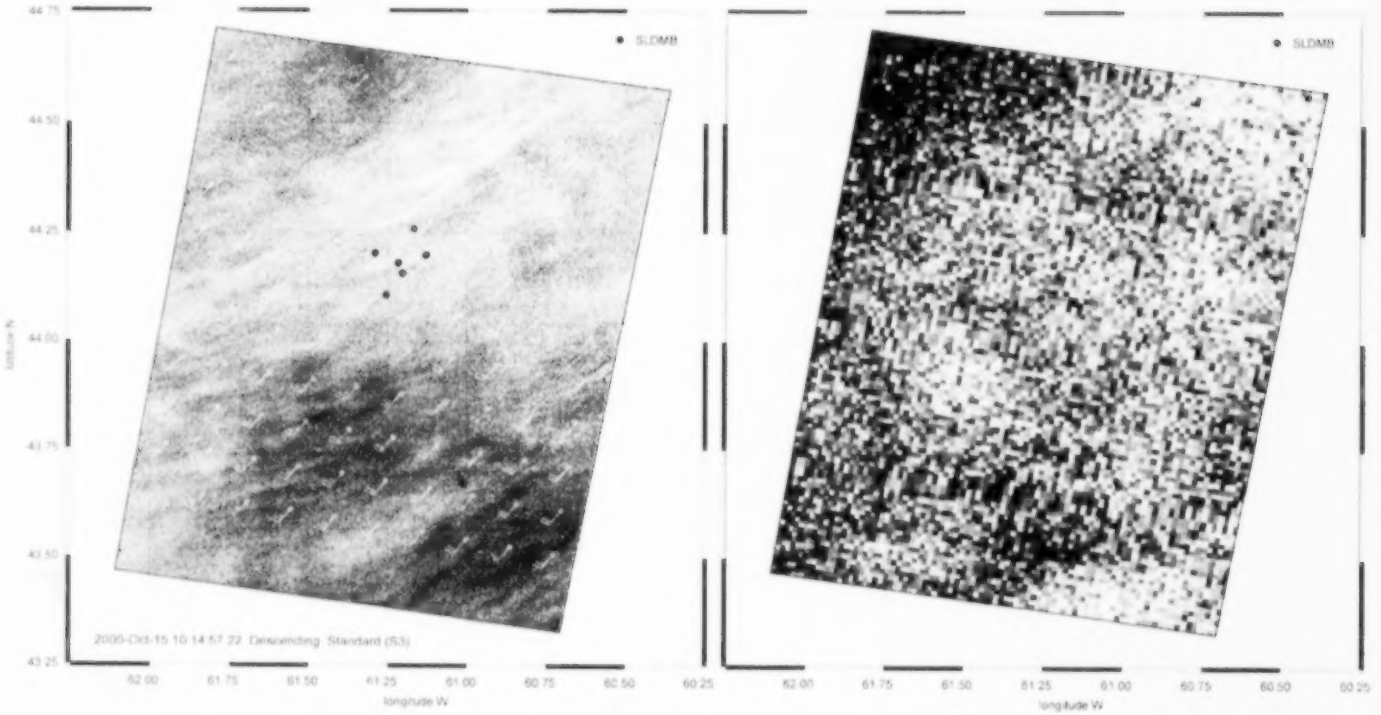

Figure 3.1b The left graphic shows the positions of SLDMBs (red dots) during the RADARSAT overpass of 15 Oct. 2000, superimposed on the SAR backscatter image and extracted wind field (yellow wind barbs). The right graphic shows the magnitude of the surface currents perpendicular to the path of the satellite, expressed as a grey scale where black corresponds to -1.1 m/s (westward) and white corresponds to 0.8 m/s (eastward).

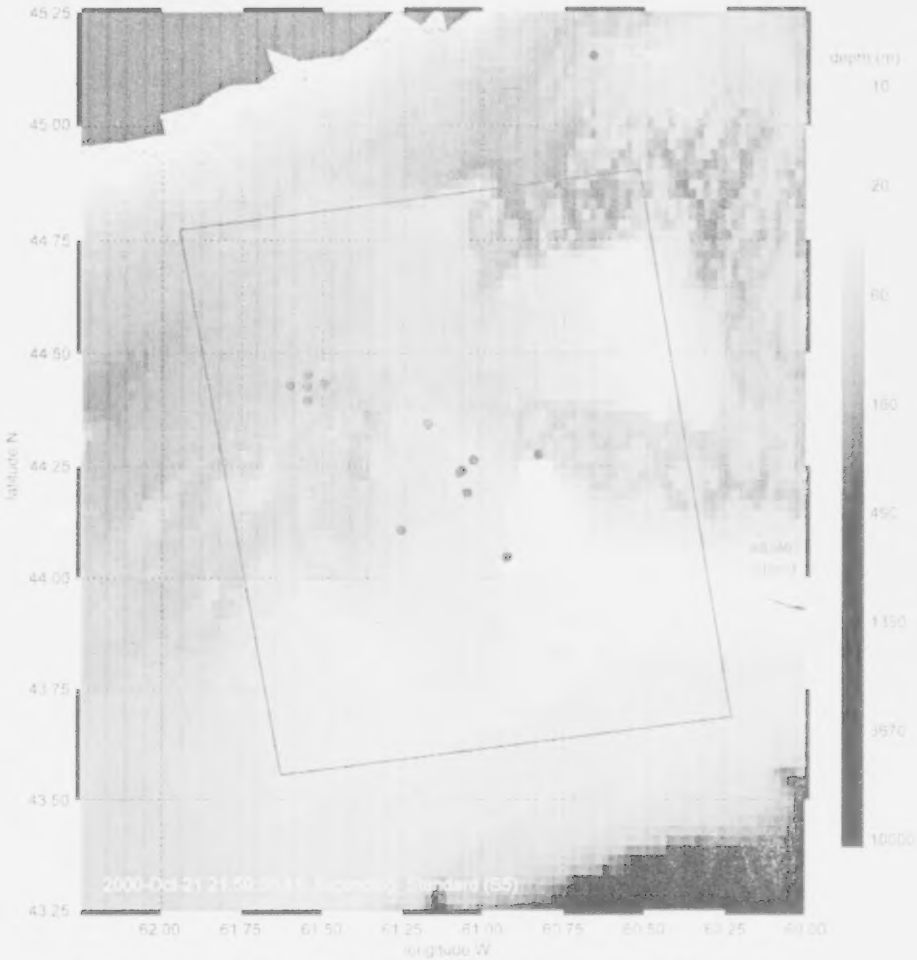

Figure 3.2a Outline of RADARSAT image area and positions of SLDMBs overlaid on bathymetry for the 21 Oct. 2000 overpass.

Table 3-2 SLDMB positions for RADARSAT overpass 21 October 2000

SLDMB (ID)	time (utc) hh:mm:ss	lat N	lon W	SLDMB (ID)	time (utc) hh:mm:ss	lat N	lon W
2391	22:00:00	44.263	-61.031	19291	22:02:00	44.428	-61.601
17309	22:01:00	44.235	-61.074	19292	22:02:00	44.343	-61.173
17311	22:01:00	44.239	-61.066	19311	22:01:00	44.190	-61.050
19268	22:00:00	44.451	-61.545	19312	22:00:00	44.046	-60.926
19276	22:01:00	44.427	-61.548	19314	22:00:00	44.275	-60.829
19281	22:01:00	44.395	-61.547	19487	22:01:00	44.106	-61.257
19290	22:00:00	44.432	-61.496				

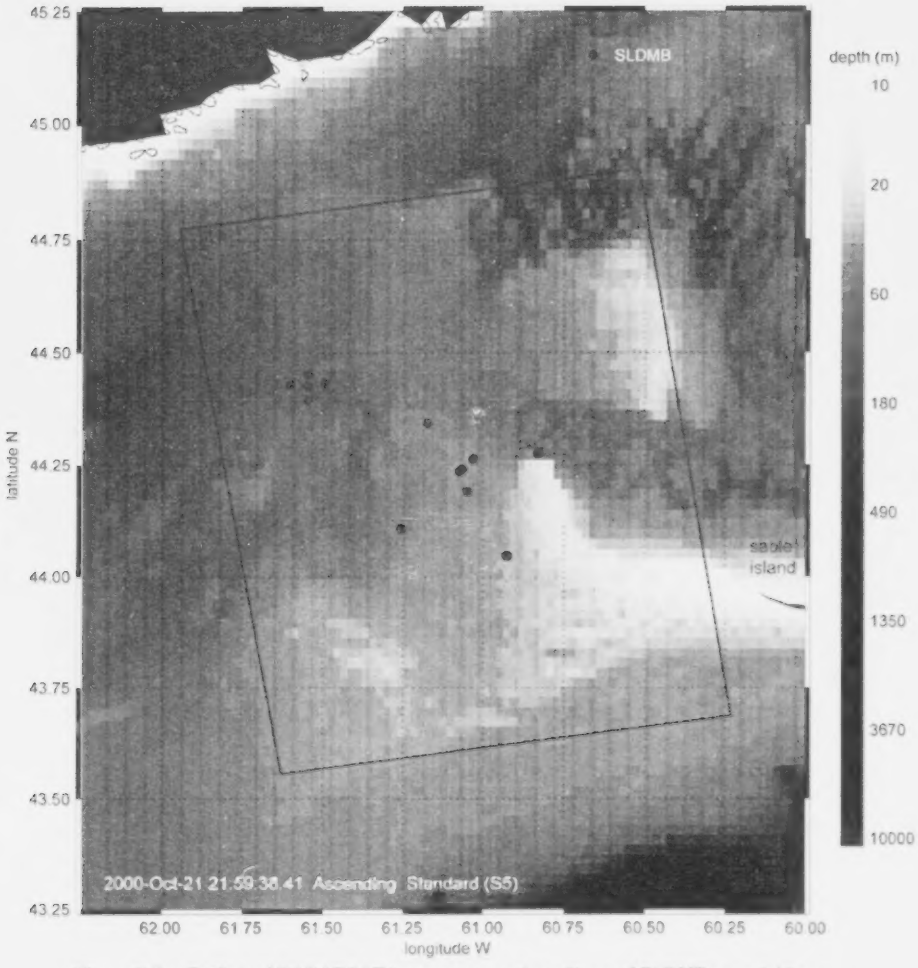

Figure 3.2a Outline of RADARSAT image area and positions of SLDMBs overlaid on bathymetry for the 21 Oct. 2000 overpass.

Table 3-2 SLDMB positions for RADARSAT overpass 21 October 2000

SLDMB (ID)	time (utc) hh:mm:ss	lat N	lon W	SLDMB (ID)	time (utc) hh:mm:ss	lat N	lon W
2391	22:00:00	44.263	-61.031	19291	22:02:00	44.428	-61.601
17309	22:01:00	44.235	-61.074	19292	22:02:00	44.343	-61.173
17311	22:01:00	44.239	-61.066	19311	22:01:00	44.190	-61.050
19268	22:00:00	44.451	-61.545	19312	22:00:00	44.046	-60.926
19276	22:01:00	44.427	-61.548	19314	22:00:00	44.275	-60.829
19281	22:01:00	44.395	-61.547	19487	22:01:00	44.106	-61.257
19290	22:00:00	44.432	-61.495	-	-	-	-

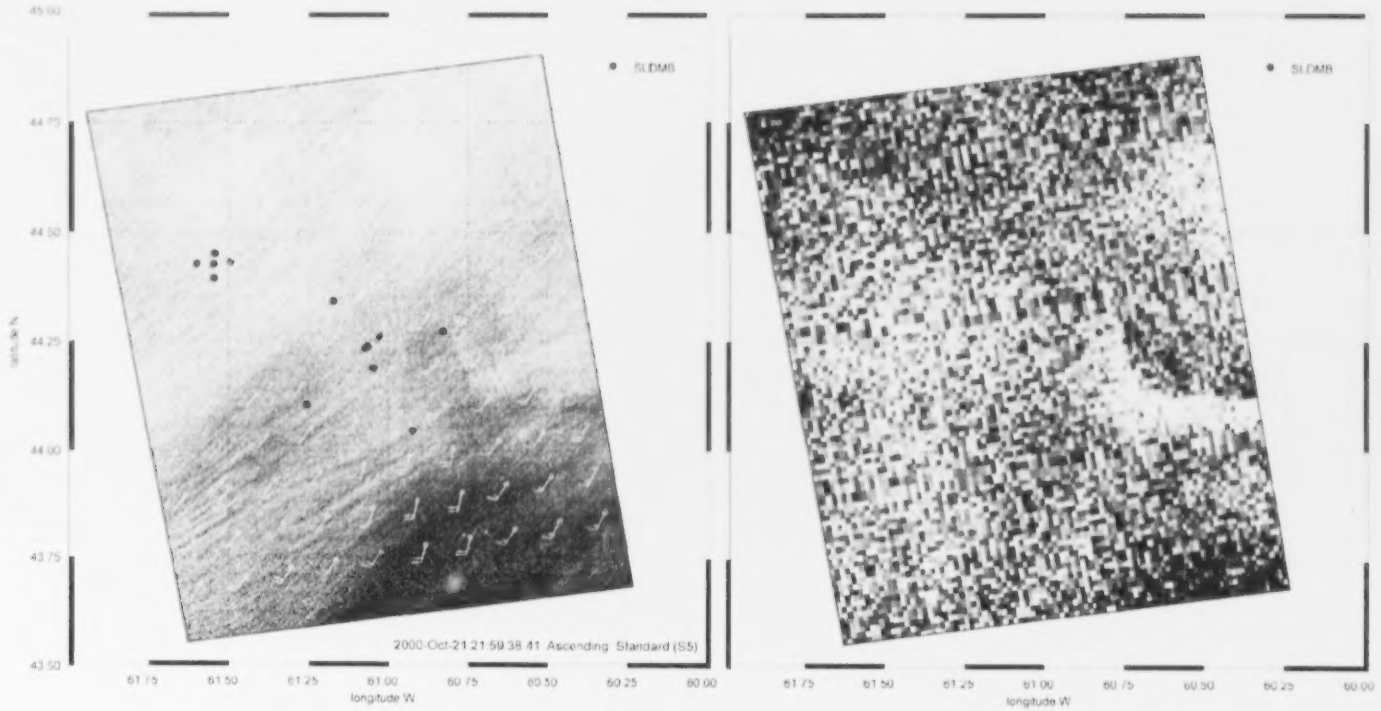

Figure 3.2b The left graphic shows the positions of SLDMBs (red dots) during the RADARSAT overpass of 21 Oct. 2000, superimposed on the SAR backscatter image and extracted wind field (yellow wind barbs). The right graphic shows the magnitude of the surface currents perpendicular to the path of the satellite, expressed as a grey scale where black corresponds to -2.1 m/s (westward) and white corresponds to 1.5 m/s (eastward).

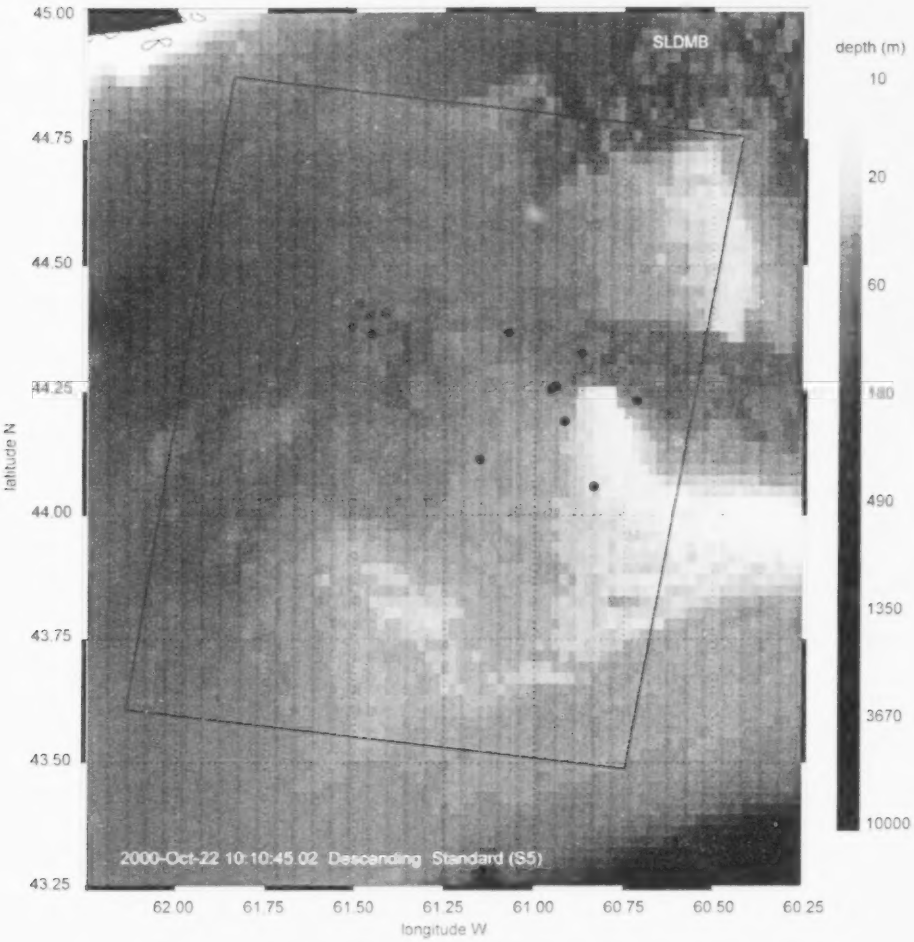

Figure 3.3a Outline of RADARSAT image area and positions of SLDMBs overlaid on bathymetry for the 22 Oct. 2000 overpass.

Table 3-3 SLDMB positions for RADARSAT overpass 22 October 2000

SLDMB (ID)	time hh:mm:ss	lat N	lon W	SLDMB (ID)	time hh:mm:ss	lat N	lon W
2391	10:02:00	44.324	-60.867	19291	10:03:00	44.378	-61.511
17309	10:01:00	44.253	-60.955	19292	10:01:00	44.366	-61.072
17311	10:01:00	44.258	-60.940	19311	10:01:00	44.189	-60.916
19268	10:01:00	44.425	-61.490	19312	10:01:00	44.058	-60.834
19276	10:01:00	44.402	-61.462	19314	10:00:00	44.231	-60.715
19281	10:03:00	44.363	-61.456	19487	10:02:00	44.112	-61.151
19290	10:02:00	44.406	-61.417	-	-	-	-

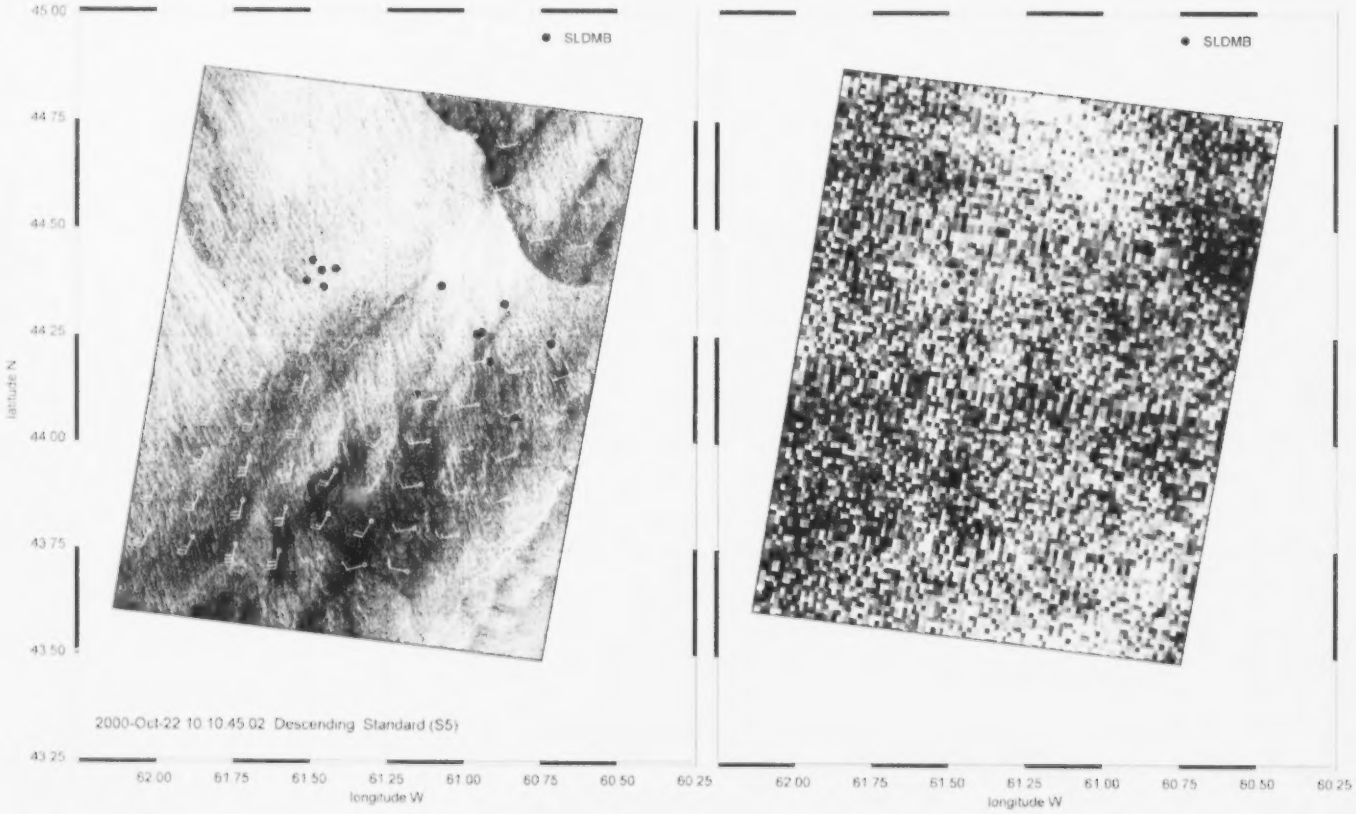

Figure 3.3b The left graphic shows the positions of SLDMBs (red dots) during the RADARSAT overpass of 22 Oct. 2000, superimposed on the SAR backscatter image and extracted wind field (yellow wind barbs). The right graphic shows the magnitude of the surface currents perpendicular to the path of the satellite, expressed as a grey scale where black corresponds to -1.9 m/s (westward) and white corresponds to 2.3 m/s (eastward).

4. Results

The *in situ* surface currents derived from the SLDMB positions and the remotely sensed currents based on the Doppler shift of the RADARSAT-1 images are presented in Tables 4-1 to 4-3. The remotely sensed currents are plotted against the component of the *in situ* currents that are perpendicular to the satellite path in Fig. 4.1. The figure shows the disappointing result that there is little or no correlation between the remotely sensed and *in situ* currents. The correlation coefficients of linear regressions are all below 0.5. The Oct.15 and 22 data actually resulted in negative correlations of -0.46 and -0.25, respectively. The correlation coefficient was +0.35 for Oct. 21.

An F-test (used to test if the variances of two populations are equal) demonstrated that the variances of the remotely sensed and *in situ* current values are significantly different for Oct. 21 and 22, with probabilities of only 0.01 and 0.32 that the variances are equal. The Oct. 15 data has a somewhat higher F-test result of 0.71 which is expected since that set has the highest correlation (although the correlation was negative). The RMS difference between remotely sensed and *in situ* currents for Oct. 15, 21 and 22 are 0.273 m/s, 0.381 m/s and 0.141 m/s, respectively. These values are approximately the same as the error specification of the process [Ref. 3] and they are of the same order as the actual currents in the study area.

For the three RADARSAT-1 passes, the *in situ* current magnitudes ranged from 0.154 m/s to 0.744 m/s. The components of the *in situ* currents perpendicular to the satellite path ranged from -0.081 m/s to 0.743 m/s, with a mean of 0.246 m/s and a standard deviation of 0.227 m/s. The remotely sensed current values corresponding to SLDMB measurements have a mean of 0.092 m/s and a standard deviation of 0.179 m/s. Since the range of values of the remotely sensed and *in situ* currents are similar, the lack of correlation between the two data sets is believed to be due to the presence of noise in one or both of the data sets.

The measured current directions were promising for Oct. 15 and 21, as they were generally perpendicular to the satellite path. However, this did not result in better agreement between the remotely sensed and *in situ* currents. The *in situ* currents on Oct. 22 were nearly parallel with the satellite path so the perpendicular components were very small and well below the noise floor of the Doppler extraction process.

In the study of Ref. 3, a bi-linear trend was removed from the remotely sensed and *in situ* current data which allowed a more accurate relationship to be established. This was not possible with the data from the present study. Several linear and 2nd order polynomials were fitted to the data in an attempt to identify a trend but the two data sets proved to be too statistical dissimilar.

Based on recent analysis of Envisat wave mode data, it has been shown that line-of-sight Doppler variations can be associated with a variety of local environmental parameters, including surface currents, surface wind, and even waves. For example, Chapron et al. [Ref. 7] found a strong correlation between the Doppler centroid anomaly and the wind vector, with surface currents dominating the Doppler centroid anomaly for low wind conditions only. In fact, they proposed that, in general, the sign of the Doppler anomaly could be used to resolve the ambiguity in SAR-derived wind direction. Inspection of the images acquired for our study suggests higher wind conditions were present in each case. Therefore, it is perhaps not surprising that we found the correlation between the Doppler anomaly and the measured surface current to be low, especially for the low surface currents that are present on the Scotian Shelf.

Given the lack of correlation between the remotely sensed and *in situ* current values, and the known accuracy limitations of the Doppler inversion process, it may be concluded that the inversion process is not accurate enough to measure the relatively low currents found on the Scotian Shelf.

Table 4-1 *in situ* and remotely sensed surface currents
October 15, 2000 10:14:53 S3/Descending

SLDMB	time (utc)	position		SLDMB speed	SLDMB dirn	SLDMB p.comp.	Doppler
(ID)	hh:mm:ss	lat N	lon W	(m/s)	(deg)	(m/s)	(m/s)
17751	10:03:00	43.684	-61.020	0.456	10.9	0.000	0.331
17846	10:01:00	43.671	-61.012	0.496	5.2	-0.050	0.042
17970	10:06:00	44.156	-61.204	0.290	77.9	0.267	-0.001
17971	10:05:00	44.201	-61.292	0.384	55.1	0.268	0.189
17972	10:06:00	44.106	-61.257	0.282	70.8	0.244	0.179
17973	10:06:00	44.198	-61.131	0.286	70.8	0.247	0.248
2332	10:01:00	44.259	-61.169	0.501	64.0	0.400	-0.225
2333	10:02:00	44.180	-61.218	0.263	83.4	0.251	0.175

Table 4-2 *in situ* and remotely sensed surface currents
October 21, 2000 21:59:34 S5/Ascending

SLDMB	time (utc)	position		SLDMB speed	SLDMB dirn	SLDMB p.comp.	Doppler
(ID)	hh:mm:ss	lat N	lon W	(m/s)	(deg)	(m/s)	(m/s)
2391	22:00:00	44.263	-61.031	0.641	57.4	0.592	0.225
17309	22:01:00	44.235	-61.074	0.453	61.5	0.430	-0.420
17311	22:01:00	44.239	-61.066	0.480	67.3	0.468	0.208
19268	22:00:00	44.451	-61.545	0.487	90.0	0.479	0.138
19276	22:01:00	44.427	-61.548	0.450	78.7	0.449	0.363
19281	22:01:00	44.395	-61.547	0.408	76.9	0.407	0.296
19290	22:00:00	44.432	-61.495	0.453	76.9	0.452	0.269
19291	22:02:00	44.428	-61.601	0.361	90.0	0.355	0.212
19292	22:02:00	44.343	-61.173	0.491	59.1	0.459	0.215
19311	22:01:00	44.190	-61.050	0.477	68.3	0.470	0.034
19312	22:00:00	44.046	-60.926	0.569	80.1	0.569	0.163
19314	22:00:00	44.275	-60.829	0.744	82.0	0.744	0.428
19487	22:01:00	44.106	-61.257	0.463	65.1	0.448	-0.060

Table 4-3 *in situ* and remotely sensed surface currents
October 22, 2000 10:10:39 S5/Descending

SLDMB	time (utc)	position		SLDMB speed	SLDMB dirn	SLDMB p.comp.	Doppler
(ID)	hh:mm:ss	lat N	lon W	(m/s)	(deg)	(m/s)	(m/s)
2391	10:02:00	44.324	-60.867	0.330	156.8	0.182	-0.223
17309	10:01:00	44.253	-60.955	0.154	180.0	0.027	-0.071
17311	10:01:00	44.258	-60.940	0.197	160.3	0.098	0.046
19268	10:01:00	44.425	-61.490	0.272	193.4	-0.015	-0.099
19276	10:01:00	44.402	-61.462	0.197	199.7	-0.033	0.091
19281	10:03:00	44.363	-61.456	0.161	180.0	0.029	0.051
19290	10:02:00	44.406	-61.417	0.308	205.4	-0.081	-0.054
19291	10:03:00	44.378	-61.511	0.272	193.4	-0.015	0.095
19292	10:01:00	44.366	-61.072	0.197	199.7	-0.032	0.038
19311	10:01:00	44.189	-60.916	0.301	166.6	0.120	-0.060
19312	10:01:00	44.058	-60.834	0.195	180.0	0.035	0.092
19314	10:00:00	44.231	-60.715	0.318	166.6	0.127	0.162
19487	10:02:00	44.112	-61.151	0.272	193.4	-0.016	0.035

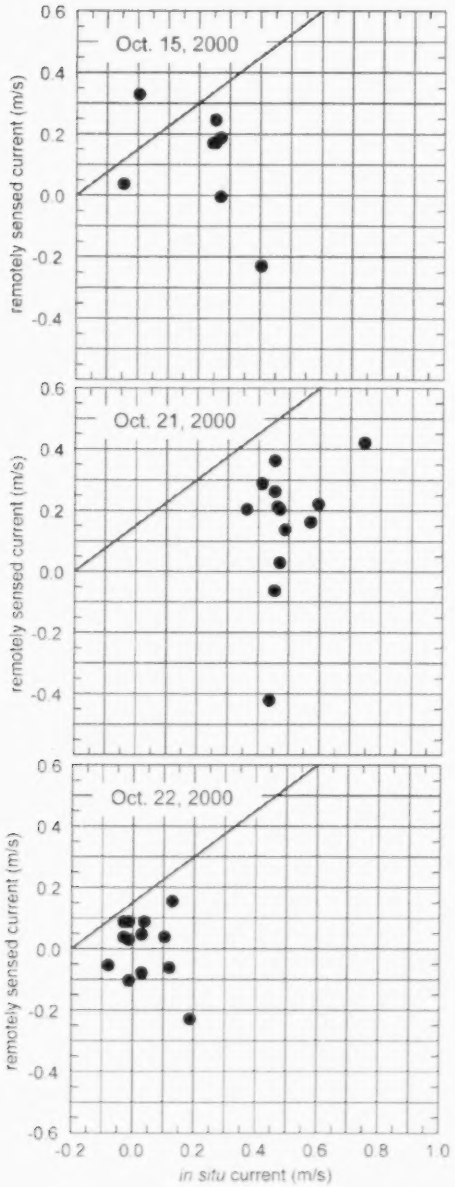

Figure 4.1 Scatter plots of remotely sensed surface current magnitude versus in situ *current component perpendicular to satellite path, determined from SLDMBs. Data along the unity lines (shown in red) would indicate perfect agreement between the remotely sensed and* in situ *values.*

5. Summary

Remotely sensed measurements of sea surface temperature and wind are standard, high quality oceanographic data products that are widely available for assimilation into numerical ocean models. However, ocean currents provide better information content for models than temperature or wind. Therefore, a means to remotely sense ocean currents from space would be an extremely valuable resource for the ocean modelling community.

Van der Kooij [Ref. 3] demonstrated successful surface current extraction from RADARSAT-1 and ERS-1 SAR imagery over the Gulf Stream.The estimated accuracy of the process was reported to be between 0.2-0.3 m/s. Since the Gulf Stream study area had surface currents up to 2.5 m/s, useful current estimates were demonstrated. Our Scotian Shelf study area had mean *in situ* surface currents of only 0.25 m/s which is within the range of the accuracy of the current extraction process. Therefore, we conclude that the surface currents in this study are at or below the noise floor of the current extraction process. Since the accuracy of *in situ* surface currents derived from SLDMBs is estimated to be better than 0.05 m/s, the lack of correlation between the remotely sensed and *in situ* currents is believed to be due to error in the remotely sensed values.

The quality of the Doppler data in the three scenes studied, was good, indicating that the Doppler centroid anomaly calculations were derived from areas with a high signal-to-noise ratio. However, the results of this work indicate that ocean surface currents derived from RADARSAT-1 using the approach of Ref. 3 are not sufficiently accurate for use over the Scotian Shelf test area.

It may be possible to demonstrate successful surface current sensing for the Scotian Shelf with existing technology by studying other areas with higher currents. For example the Nova Scotia current which moves southward along the south coast of Nova Scotia has speeds that exceed 1 m/s.

Future studies should be conducted with greater numbers of SLDMBs. The 8 to 13 SLDMBs available in the imagery of the present study was not sufficient to allow adequate calibration of the Doppler derived velocities. As well, future studies should involve the refining of beam mode selection for the optimum combination of high signal-to- noise ratio and large Doppler shifts.

The launch of ENVISAT in March, 2002 and RADARSAT-2 in 2005 may allow fo: an improvement of the performance of the current extraction process, as the quality of the SAR sensors on these satellites is better than those currently being used. The multi-polarimetric nature of both the ENVISAT and RADARSAT-2 SARs should allow higher signal to noise ratios to be obtained for Doppler shift detection, especially in the VV (vertical send / vertical receive) mode. However, recent analysis of Envisat wave mode data (Ref. 7) indicates that the Doppler centroid anomaly is sensitive to local winds which contaminate the surface current information, therefore the current extraction process used here may only be valid for low wind conditions.

References

1. Raney, K. R., "Synthetic aperture imaging of radar and moving targets", IEEE Trans. On Aerospace and Electronic Systems, Vol. AES-7, No.3, 499-505 (1971).

2. Shuchman, R., "The feasibility of measurement of ocean current detection using SAR data", Proc. of the 13th Intl. Symposium on Remote Sensing of the Environment, Ann Arbor, 93-103 (1979).

3. Van der Kooij, M., W. Hughes and S. Sato, "Doppler current velocity measurements: A new dimension in spaceborne SAR data", 2nd Intl. Symposium on Operationalization of Remote Sensing, Enschede, The Netherlands, 16-20 August (1999).

4. Coffin, M., "Visualization and analysis of oceanographic data from Scotian Shelf trials Q267 and Q255", DRDC Atlantic Co-op work term report, April 2003.

5. Stockhausen, J, "Evaluation of current-sensing capability of RADARSAT-1", Contract report, Contract W7707-00-8816, DRDC Atlantic (2001).

6. Vachon, P. W., and F. W. Dobson, "Wind retrieval from RADARSAT SAR images: Selection of a suitable C-band HH polarization wind retrieval model", Can. J. Rem. Sens., Vol. 26, No. 4, 306-313, (2000).

7. Chapron, B., F. Collard, and V. Kerbaol, "Satellite synthetic aperture radar sea surface Doppler measurements", to appear, Proc. 2nd Workshop on Coastal and Marine Applications of SAR, Svalbard, Norway, 8 to 12 September 2003. Available: http://fermi.jhuapl.edu/meetings/svalbard_2003/chapron.pdf

Distribution list

List Part 1:

2	DRDC Atlantic library file copies
4	DRDC Atlantic library (spares)
4	Dan Hutt (author), 2 hardcopies, 2 CDs
2	Don Mosher (author), 1 hardcopies, 1 CD
1	John Osler, GL/Ocean Sensing and Modelling Group
1	Paul Hines, Ocean Sensing and Modelling Group
1	Neil Sponagle, H/Underwater Sensing
1	Zahir Daya, Integrated Signature Management Group
1	Boris Vasiliev, Integrated Signature Management Group
1	Troy Richards, Integrated Signature Management Group
1	Courtney Greene, Integrated Signature Management Group
19	total list part 1

List Part 2: distributed by DRDKIM 3

1 ADM(S&T)/DRDKIM 3
National Defence Headquarters
305 Rideau Street
Ottawa, Ontario, K1A 0K2

1 Jeff Stockhausen (author)
Helical Systems Limited
1 Research Drive
Dartmouth, NS
Canada B2Y 4M9

1 Dr. Jake Tunaley
1 Dr. Paris Vachon (author)
Defence R&D Canada - Ottawa
3701 Carling Avenue
Ottawa, Ontario, K1A 0Z4

1 LCdr Andy Cameron, D MetOc 2-2
National Defence Headquarters
Lorne building, 90 Elgin Street
Ottawa, Ontario, K1A 0K2

1 Lt(N) Shawn Donohue, Fleet Tactical Oceanographer
MARLANT/MetOc (N35-2)
MetOc Halifax, Building D201
PO Box 99000 Stn. Forces
Halifax, Nova Scotia, B3K 5X5

1 LCdr Robert Quinn, D Polar Epsilon
Directorate of Space Development
MGen George R. Pearkes Building
Ottawa, Ontario, K1A 0K2

1 Prof. Keith Thompson
Dalhousie University
Department of Oceanography
Halifax, Nova Scotia
Canada, B3H 4J1

1 Mac Macleod
Seimac Inc.
271 Brownlow Ave.
Dartmouth, Nova Scotia
Canada, B3B 1W6

1 Dr. Marco van der Kooij
Atlantis scientific
20 Colonnade Road, Suite 110
Nepean, Ontario
Canada, K2E 7M6

1 Dr. Roger Gauss
NRL Code 7144
4555 Overlook Ave., SW
Washington, DC
United States, 20375-5350

11 total list part 2

30 Total copies required

DOCUMENT CONTROL DATA

(Security classification of title, body of abstract and indexing annotation must be entered when the overall document is classified)

1. ORIGINATOR (the name and address of the organization preparing the document. Organizations for whom the document was prepared, e.g. Centre sponsoring a contractor's report, or tasking agency, are entered in section 8.)

DRDC Atlantic

2. SECURITY CLASSIFICATION (overall security classification of the document including special warning terms if applicable).

UNCLASSIFIED

3. TITLE (the complete document title as indicated on the title page. Its classification should be indicated by the appropriate abbreviation (S,C,R or U) in parentheses after the title).

Capability of RADARSAT-1 for estimation of ocean surface current on the Scotian Shelf

4. AUTHORS (Last name, first name, middle initial. If military, show rank, e.g. Doe, Maj. John E.)

Hutt, D., Stockhausen, J., Vachon, P. W. and Mosher, D.

5. DATE OF PUBLICATION (month and year of publication of document)	6a. NO. OF PAGES (total containing information Include Annexes, Appendices, etc).	6b. NO. OF REFS (total cited in document)
December 2003	23	7

7. DESCRIPTIVE NOTES (the category of the document, e.g. technical report, technical note or memorandum. If appropriate, enter the type of report, e.g. interim, progress, summary, annual or final. Give the inclusive dates when a specific reporting period is covered).

Technical memorandum

8. SPONSORING ACTIVITY (the name of the department project office or laboratory sponsoring the research and development. Include address).

Defence R&D Canada – Atlantic
PO Box 1012
Dartmouth, NS, Canada B2Y 3Z7

9a. PROJECT OR GRANT NO. (if appropriate, the applicable research and development project or grant number under which the document was written. Please specify whether project or grant).	9b. CONTRACT NO. (if appropriate, the applicable number under which the document was written).
TIF 1CA16	N/A

10a ORIGINATOR'S DOCUMENT NUMBER (the official document number by which the document is identified by the originating activity. This number must be unique to this document.)	10b OTHER DOCUMENT NOs. (Any other numbers which may be assigned this document either by the originator or by the sponsor.)
DRDC Atlantic TM 2003-268	DRDC Atlantic

11. DOCUMENT AVAILABILITY (any limitations on further dissemination of the document, other than those imposed by security classification)

(x) Unlimited distribution
( ) Defence departments and defence contractors; further distribution only as approved
( ) Defence departments and Canadian defence contractors; further distribution only as approved
( ) Government departments and agencies; further distribution only as approved
( ) Defence departments; further distribution only as approved
( ) Other (please specify):

12. DOCUMENT ANNOUNCEMENT (any limitation to the bibliographic announcement of this document. This will normally correspond to the Document Availability (11). However, where further distribution (beyond the audience specified in (11) is possible, a wider announcement audience may be selected).

13. ABSTRACT (a brief and factual summary of the document. It may also appear elsewhere in the body of the document itself. It is highly desirable that the abstract of classified documents be unclassified. Each paragraph of the abstract shall begin with an indication of the security classification of the information in the paragraph (unless the document itself is unclassified) represented as (S), (C), (R), or (U). It is not necessary to include here abstracts in both official languages unless the text is bilingual).

(U) Doppler shifts in space-based SAR data are due to movement of objects in the image area. These frequency shifts are most obvious in fast moving point targets such as ships. However, an area target such as the sea surface can also cause a measurable Doppler shift from which ocean surface currents can be estimated. We compare surface currents derived from three standard mode Radarsat1 scenes over the Scotian shelf to in situ currents measured with 20 self-locating datum marker buoys (SLDMBs). The SLDMBs are assumed to drift with the local surface current, and their locations, obtained every 30 minutes via Argos satellite, are used to calculate the current. Three Radarsat1 scenes were processed by Atlantis Scientific, of Ottawa, Canada to obtain the component of the surface current vector perpendicular to the path of the satellite. The results show that the noise in the derived Doppler shift was comparable to the Doppler shift expected from the relatively low surface currents prevalent on the Scotian Shelf. While it was concluc d that present space-based SAR technology cannot provide accurate surface current data for Scotian Shelf conditions, the methodology and results provide a useful metric by which future SAR systems can be evaluated.

14. KEYWORDS, DESCRIPTORS or IDENTIFIERS (technically meaningful terms or short phrases that characterize a document and could be helpful in cataloguing the document. They should be selected so that no security classification is required. Identifiers, such as equipment model designation, trade name, military project code name, geographic location may also be included. If possible keywords should be selected from a published thesaurus. e.g. Thesaurus of Engineering and Scientific Terms (TEST) and that thesaurus-identified. If it not possible to select indexing terms which are Unclassified, the classification of each should be indicated as with the title).

Remote sensing
RADARSAT
surface currents
Underwater acoustics